

# Spurious Shear from the Atmosphere in Ground-Based Weak Lensing Observations

D. Wittman<sup>1</sup>

## ABSTRACT

Weak lensing observations have the potential to be even more powerful than cosmic microwave background (CMB) observations in constraining cosmological parameters. However, the practical limits to weak lensing observations are not known. Most theoretical studies of weak lensing constraints on cosmology assume that the only limits are shot noise on small scales, and cosmic variance on large scales. For future large surveys, shot noise will be so low that other, systematic errors will likely dominate. Here we examine a potential source of additive systematic error for ground-based observations: spurious power induced by the atmosphere. We show that this limit will not be a significant factor even in future massive surveys such as LSST.

*Subject headings:* gravitational lensing — atmospheric effects — surveys

## 1. Introduction

Weak lensing by large-scale structure imprints correlated ellipticities onto images of distant galaxies. This cosmic shear effect was predicted in the 1960's (Kristian & Sachs 1966), but not detected until 2000 (Wittman *et al.* 2000; van Waerbeke *et al.* 2000; Bacon *et al.* 2000; Kaiser, Wilson & Luppino 2000). Cosmic shear can provide a relatively clean probe of cosmological parameters because it depends only on the mass distribution and not on detailed astrophysics such as galaxy bias or gas heating and cooling. The observational state of the art has rapidly progressed to quantitative constraints on dark energy (*e.g.* Jarvis *et al.* 2005). Future large surveys such as LSST (Tyson *et al.* 2003) and SNAP (Refregier *et al.* 2004) are intended to make these constraints precise.

However, the practical limits to weak lensing accuracy are not well known. The limits which are well known are shot noise on small scales, and cosmic variance on large scales. However, shot noise is so low for future large surveys that other, systematic errors will

---

<sup>1</sup>Physics Department, University of California, Davis, CA 95616; dwittman@physics.ucdavis.edu

likely dominate. Likely sources of systematics include shear calibration, photometric redshift errors, spurious power from instrumental and atmospheric effects, and perhaps intrinsic alignments. Some of these have already been addressed in the literature. Shear calibration, probably the most important multiplicative effect, includes a correction for the dilution of shear by the isotropic smearing of the point-spread function (PSF) by the atmosphere. Heymans *et al.* (2005) examined these errors empirically, by conducting blind analyses of a synthetic dataset, using various shear calibration methods. The accuracy of the best current methods was good to  $\sim 1\%$ . Guzik & Bernstein (2005) examined the effect of spatially varying calibration errors and concluded that limiting spatial variations in calibration to 3% rms would be sufficient to keep systematic errors below statistical errors in future surveys like LSST. Ma *et al.* (2005) explored the mitigation of photometric redshift errors in tomography, and King (2005) did the same for intrinsic alignments, but neither tried to predict the actual level of error.

Here we quantify the likely level of an additive systematic in ground-based observations: spurious power from the atmosphere. A fixed realization of atmospheric turbulence imparts position-dependent ellipticity variations onto the PSF. If not removed, this will result in additive spurious power. With  $\sim 1$  PSF star arcmin $^{-2}$  available to diagnose the PSF, and atmospheric power predicted on smaller scales, this effect surely cannot be removed completely. Of course, long exposure times average over many different realizations of atmospheric turbulence which should converge to an isotropic PSF (apart from instrumental aberrations, which can be significant). One of the goals of this paper is to measure the potential atmospheric contribution as a function of exposure time, to aid in the design of future high-precision surveys.

Every weak lensing analysis has a PSF anisotropy correction. Therefore the relevant question is not how much spurious ellipticity is induced by the atmosphere; it is how much remains after the PSF anisotropy correction. For that reason, we conduct a mock lensing analysis of a dense star field rather than rely on atmospheric modeling.

## 2. Dataset

We take the Large Synoptic Survey Telescope (LSST, Tyson *et al.* 2003) as a fiducial survey. The LSST calls for an 8.4 m telescope with a 10 deg $^2$  field of view, repeatedly surveying  $\sim 20,000$  deg $^2$  of sky in multiple optical bandpasses (*grizy*). Each field will be imaged hundreds of times in some filters, with rather short exposure times ( $\sim 15$  seconds). The motivation for this is two-fold: to provide time sampling for scientific goals other than weak lensing, and to provide the ability to “chop” the dataset against any desired variable

to identify and remove weak lensing systematics.

We have identified a real dataset which has many of the parameters required to explore spurious shear in such a survey: A set of 10- and 30-second exposures of a dense star field taken by the Subaru 8-m telescope with its prime-focus camera SuprimeCam. A dense star field is required to assess the variation of the PSF on small angular scales; the short exposures and  $\sim 0.7''$  FWHM seeing are typical of LSST; SuprimeCam has the widest field of any 8 m class telescope/imager; and the 8 m aperture is a good match. Technically, this last match may or may not be important. The expected scaling of atmosphere-induced ellipticity with aperture size cancels the expected scaling with exposure time, so that all observations of a given depth should have a similar level. However, in practice other factors may come into play. For example, if the outer scale of atmospheric turbulence is not much larger than the telescope aperture, the scaling arguments are invalid. For this dataset we do not have independent measurements of the outer scale or any other atmospheric parameters, but the 8 m aperture will minimize the risk of mismatches with the LSST dataset.

The exposures were taken on 7 May 2002 through the  $i'$  filter, at airmasses very near unity (1.003–1.012), with seeing slightly better than  $0.7''$ . The field was centered at 18:25:59.955 +21:42:19.06, with no dithering.

### 3. Analysis

An anisotropic PSF leads directly to an additive systematic in the galaxy shape measurements, and thus to spurious shear. Initial PSF anisotropy in ground-based images is typically  $\sim 5\%$ . This represents a huge “foreground” which must be removed to reveal the  $\sim 1\%$  or smaller cosmic shear signal. The steps in the PSF anisotropy correction are: identification of PSF stars; interpolation of the spatially varying PSF to the position of the galaxy in question; and correction of the galaxy shape.

The initial density of stars in these observations is  $\sim 8 \text{ arcmin}^{-2}$ . We choose a random subset of density  $0.9 \text{ arcmin}^{-2}$ , typical of current high-latitude surveys, to act as the stars available for the PSF correction. The remainder are designated as test particles to measure the residuals. These subsets are hereafter referred to as PSF stars and test stars respectively. Future surveys such as LSST may have somewhat more PSF stars available for several reasons. First, the angular resolution of ground-based observations has improved with time, as dome seeing has been minimized and better sites have been identified at great expense. It is a near certainty that LSST seeing will be better than in current wide-field surveys on older facilities; the LSST plan calls for a threshold of  $0.7''$  for data to be used in the weak

lensing analysis. This better angular resolution will allow better star/galaxy separation and a higher density of usable PSF stars. Second, a large survey can work very hard to identify more stars. The survey can perform star-galaxy separation on the best-seeing images and compile a database of PSF star positions usable in all seeing conditions, and it can use color information, not just size, to identify stars. Neither of these techniques is currently employed. The following results improve by 20—25% if the PSF star density is doubled to  $1.8 \text{ arcmin}^{-2}$ .

The next step is interpolating the PSF to the position of each galaxy or test star. Clearly the final results will depend on the effectiveness of the interpolation scheme. Typically a polynomial of order  $\sim 3$  is fit to each CCD in each exposure. More sophisticated schemes have been used to reach smaller scales for fixed patterns persisting throughout multiple exposures (Jarvis & Jain 2004), but the atmosphere is stochastic and is unlikely to be more accurately diagnosed by such a scheme. Therefore we use a simple third-order polynomial. We also tried nearest neighbor and bicubic spline interpolation, which fared slightly worse and are not presented here. The resulting limit on spurious shear is conservative because a better interpolation scheme may be found.

Figure 1 illustrates the interpolation input and output. The left panel shows the spatial variation of all the measured ellipticities in one of the ten SuprimeCam CCDs, and the center panel shows the interpolated ellipticities. At each point where the PSF is measured or interpolated, we plot a line segment at the PSF position angle, with length proportional to the PSF ellipticity. The atmosphere is not necessarily responsible for all the variation shown. However, contributions from the optics are likely to be on angular scales easily modeled by this interpolation process. Therefore we are most interested in what remains after removing this pattern.

The final step, galaxy shape correction, also has been implemented in various ways. The simplest conceptually is to measure the galaxy shape after convolving the image with a spatially varying kernel such that the final PSF is isotropic (Fischer & Tyson 1997; Kaiser 2000; Bernstein & Jarvis 2002). Here we will assume that the result of the convolution is as good as the PSF interpolation allows. This is a good assumption in practice; and in principle, if the convolution is imperfect it can be iterated until it is limited only by the PSF interpolation. Therefore we subtracted the interpolated ellipticities componentwise from the measured ellipticities of the test stars, mimicking a perfectly effective convolution step. This is illustrated by the right panel of Figure 1. Blends and other corrupted shape measurements now stand out quite clearly. Because these have no preferred orientation, they add noise but not bias to the following measurement.

Finally, we convert the residual ellipticities to shears with the standard factor of two and

compute the shear correlation functions of the corrected test stars. In reality, the conversion of PSF ellipticity to inferred spurious shear depends on the size of the galaxy relative to the PSF. If an initially circular source is resolved, its measured ellipticity will always be less than the PSF ellipticity. But for barely-resolved galaxies, the spurious ellipticity will be amplified by the subsequent correction for dilution due to the isotropic part of the PSF (variously called seeing correction, dilution correction, or shear calibration). These effects combine to make the inferred pre-seeing ellipticity equal to the PSF ellipticity for galaxies with pre-seeing size equal to the PSF size; less for larger galaxies, and more for smaller galaxies. This transition size is not atypical for galaxies used in a ground-based lensing analysis, so we apply no correction factor here, with the caveat that the impact on a real lensing survey could vary by up to a factor of  $\sim 2$ , depending on how aggressively the analysis uses barely-resolved galaxies.

The final result may be an overestimate of the atmospheric contribution, as there may be remaining unmodelled instrumental effects. In a real survey, such effects could be identified in any of several ways (principal component analysis as in Jarvis & Jain 2004, detailed optomechanical modeling of the camera, or measured on the fly with wavefront sensors) and then removed.

## 4. Results

As an estimate of the spurious power induced by the atmosphere, we plot the shear correlations of the corrected test stars in Figure 2, for both 10-second (black) and 30-second (red) exposures. In each case, only one shear component is plotted because the two components were indistinguishable. At each angular separation, the points and error bars plotted reflect the mean and rms variation across the five exposures of each duration. Note that neighboring points are highly correlated.

For vanishing angular separation, the quantity plotted in Figure 2 is equivalent to the mean-square value of the residual atmospheric shear. For  $n$  independent realizations of atmospheric turbulence, we expect this to go as  $n^{-1}$ , *i.e.*, the rms goes as  $n^{-1/2}$ . The improvement from 10-s to 30-s exposure time is more modest (a factor of 2.4 rather than 3), probably because the atmosphere has not completely decorrelated in 30 seconds. Perhaps it would be better to accumulate a longer exposure time by taking multiple short exposures, alternating fields so that the atmosphere is completely decorrelated by the time a field is revisited. To investigate this possibility, we examined a set of five consecutive 10-second exposures. The SuprimeCam read time is long enough ( $\sim 120$  seconds) that it is a fair comparison to LSST, with its fast read time and point/settle time, doing several fields

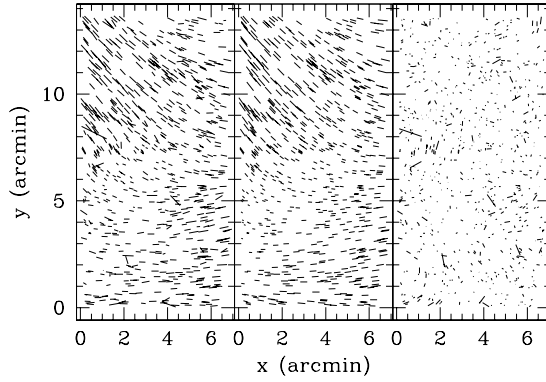


Fig. 1.— Left: PSF ellipticity map of one of the ten SuprimeCam CCDs in one 10 s exposure, using test stars ( $\sim 7 \text{ arcmin}^{-2}$ ). Center: polynomial model based on disjoint sample of  $\sim 1$  PSF star  $\text{arcmin}^{-2}$ . Right: test star residuals after model subtraction. Apart from blends and other corrupted shape measurements, the mean scalar ellipticity before subtraction is 0.07 and the maximum is 0.12, in the upper left corner. After subtraction, these numbers drop to 0.02 and 0.06.

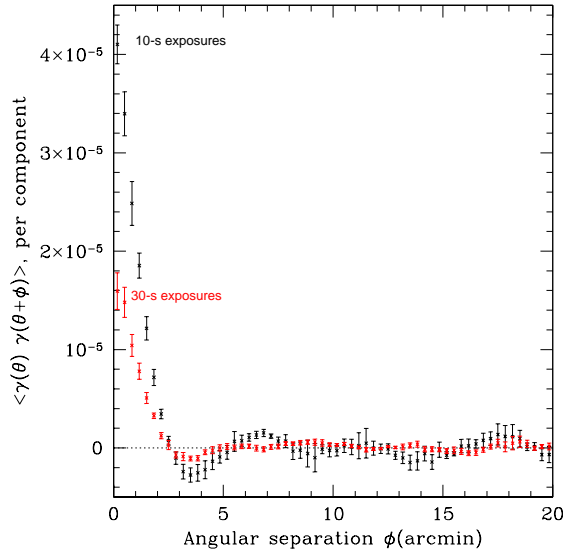


Fig. 2.— Residual shear correlations after PSF correction for 10-second (red) and 30-second (black) exposures on the Subaru telescope. In each case, only one shear component is plotted for clarity; the two components are nearly indistinguishable in their behavior. The ringing at large angular separation is an artifact of the interpolation scheme.

and coming back for a revisit. For any reasonable atmosphere, it should provide complete decorrelation. For each test star, we took the mean of the five corrected shapes as its final shape estimate. The result is shown in Figure 3, now zoomed in to small separations where the correlations are detectable. The improvement is indeed a factor of five at the smallest angular scales, but less at  $2'$  scales. One possible explanation is unmodelled instrumental effects. CCD height variations, for example, are expected at scales some fraction of a CCD size ( $7'$  in this case), but not at very small scales, where the atmosphere should dominate. The effects of CCD height variations would not average down at all with multiple undithered exposures, but with sufficient effort they could be calibrated and removed from a large survey.

The LSST dataset will contain hundreds of visits to each field in each of two bandpasses which will be observed only in good seeing ( $r$  and  $i$ ). Therefore the spurious shear correlation from the atmosphere will be on the order of  $10^{-7}$  at  $1'$  scales. This is 3–4 orders of magnitude below the expected lensing shear correlation per component, which is  $4 \times 10^{-4}$  for an effective source redshift of 1.0 in a  $\Lambda$ CDM universe (Jain & Seljak 1997). This is the angular scale at which the spurious shear is at a maximum relative to the expected lensing signal, at least in the range of scales measured here. The expected shear correlation from lensing does not decline any more rapidly with angular scale than do these measurements, so there is little reason to think that spurious shear from the atmosphere will become a significant factor at any angular scale. The projected spurious shear from the atmosphere is also much smaller than the expected LSST statistical errors, which are as good as  $\sim 1\%$  in any one redshift bin and angular scale.

## 5. Summary and Discussion

We have measured residual shear correlations in LSST-like short exposures, after PSF anisotropy correction using current algorithms and a conservative density of PSF stars. To the extent that the standard PSF anisotropy correction models away instrumental effects, the residual correlations can be interpreted as coming from atmospheric turbulence. Because it is unlikely that all instrumental effects have been modeled perfectly, this can be taken as a conservative upper estimate of spurious shear from the atmosphere at unity airmass. For a real LSST-like survey, airmass effects would increase the spurious shear by less than a factor of two. Also, depending on how aggressively future surveys attempt to use barely resolved galaxies, the following results could go up or down by a factor of two.

At  $1'$  scales, where the spurious shear is at its maximum relative to the expected lensing signal, a single 10 s exposure exhibits residual correlations a factor of  $\sim 20$  smaller than the lensing signal. For longer single exposures up to 30 s, the spurious shear correlations

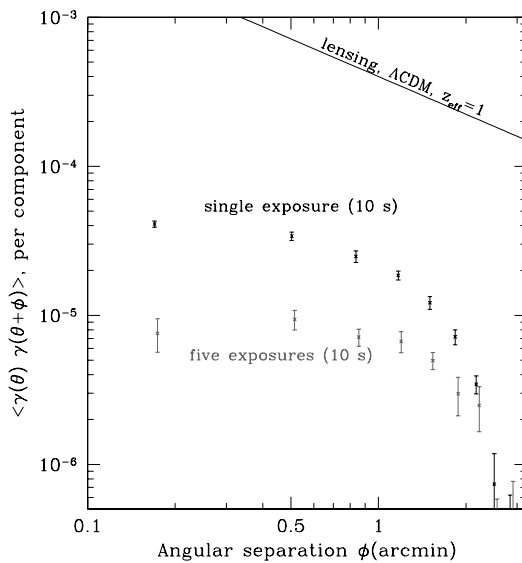


Fig. 3.— Decrease of residual shear correlations from a single 10 s exposure (black) to a coadd of five 10 s exposures (gray, and slightly offset horizontally for clarity). The expected fivefold decrease is realized at some, but not all, angular scales, possibly due to unmodelled instrumental effects. LSST plans to take 200 exposures in each filter for each field. The expected lensing signal is shown for an effective source redshift of unity and a  $\Lambda$ CDM universe (Jain & Seljak 1997).



decrease somewhat more slowly than the inverse of the exposure time. For coadds of multiple independent exposures separated by  $\sim 120$  s, the correlations at scales  $< 1'$  decrease linearly with the number of exposures, *i.e.* the rms spurious shear goes as  $n^{-1/2}$ . At larger scales, the observed decrease is smaller. However, with no reason to believe that the temporal nature of the atmosphere is a function of angular scale, unmodelled instrumental artifacts at a fixed angular scale must be responsible for this behavior. In a real survey, such artifacts could be diagnosed and modeled out. In fact, a strategy as simple as dithering could change this systematic into a random error which would average down. With hundreds of independent exposures, the residual correlations in the coadded LSST dataset will be 3–4 orders of magnitude less than the signal and comfortably less than the shot noise.

Spurious shear from the atmosphere will not be a major systematic in ground-based lensing surveys. Shear calibration, photometric redshift errors, and their spatial variations are likely to be more important sources of systematics. Heymans *et al.* (2005) showed that the best current shear calibrations are good to  $\sim 1\%$ . Overall shear calibration could be treated as a nuisance parameter in the analysis with a significant penalty, about a factor of two degradation in the resulting cosmological parameter errors (Huterer *et al.* 2005). Spatial variations in the calibration cannot be treated this way even in principle, and will have to be controlled to  $\sim 3\%$  (Guzik & Bernstein 2005), which is probably achievable in future ground-based surveys. For photometric redshifts, Ma *et al.* (2005) found that the bias and scatter in each redshift bin of width 0.1 must be known to better than about 0.003–0.01 to avoid more than a 50% increase in dark energy parameter errors. This will be a challenge for deep surveys whose imaging goes beyond the capabilities of other facilities to provide supporting spectroscopy. Finally, at small scales ( $l > 1000$ ), theoretical uncertainty in predicting the shear power spectrum due to baryonic effects may be a source of uncertainty at the  $\sim 1\%$  level (Zhan & Knox 2004).

Another potentially important systematic is spurious shear due to the telescope and camera. Comparisons to current instruments are likely to be misleading because future surveys will be the first ones built from the ground up to minimize lensing systematics. The LSST camera, for example, will have wavefront sensors throughout the focal plane so that the exact state of the optics will be known as a function of time. Both the pupil and the camera will rotate with respect to the sky, providing another important way to diagnose and reduce systematics. We cannot yet estimate the level of spurious shear due to the telescope and camera, but because these items are testable in situ, it seems likely that they will be controlled at least as well as shear and photometric calibration, which depend on observing conditions which are not under direct control. The dataset of hundreds of exposures of each field will be critical for analyzing the effects of observing conditions and thus improving the limits on spatial variations of shear calibration and photometric calibration.

We thank Vera Margoniner, Garrett Jernigan, Tony Tyson, Steve Kahn, and John Peterson for valuable discussions. Based on data collected at Subaru Telescope and obtained from the SMOKA science archive at Astronomical Data Analysis Center, which is operated by the National Astronomical Observatory of Japan.

## REFERENCES

- Bacon, D. J., Refregier, A. R., & Ellis, R. S. 2000, *MNRAS*, 318, 625
- Bernstein, G. M., & Jarvis, M. 2002, *AJ*, 123, 583
- Fischer, P., & Tyson, J. A. 1997, *AJ*, 114, 14
- Guzik, J., & Bernstein, G. 2005, *ArXiv Astrophysics e-prints*, arXiv:astro-ph/0507546
- Huterer, D., Takada, M., Bernstein, G., & Jain, B. 2005, *ArXiv Astrophysics e-prints*, arXiv:astro-ph/0506030
- Kristian, J., & Sachs, R. K. 1966, *ApJ*, 143, 379
- Kristian, J. 1967, *ApJ*, 147, 864
- Heymans, C., et al. 2005, *ArXiv Astrophysics e-prints*, arXiv:astro-ph/0506112
- Jain, B., & Seljak, U. 1997, *ApJ*, 484, 560
- Jarvis, M., & Jain, B. 2004, *ArXiv Astrophysics e-prints*, arXiv:astro-ph/0412234
- Jarvis, M., Jain, B., Bernstein, G., & Dolney, D. 2005, *ArXiv Astrophysics e-prints*, arXiv:astro-ph/0502243
- Kaiser, N., Wilson, G. & Luppino, G. 2000, *ArXiv Astrophysics e-prints*, arXiv:astro-ph/0003338
- Kaiser, N. 2000, *ApJ*, 537, 555
- King, L. 2005, *ArXiv Astrophysics e-prints*, arXiv:astro-ph/0506441
- Ma, Z., Hu, W., & Huterer, D. 2005, *ArXiv Astrophysics e-prints*, arXiv:astro-ph/0506614
- Refregier, A., et al. 2004, *AJ*, 127, 3102
- Tyson, J. A., Wittman, D. M., Hennawi, J. F., & Spergel, D. N. 2003, *Nuclear Physics B Proceedings Supplements*, 124, 21

Van Waerbeke, L., et al. 2000, *A&A*, 358, 30

Wittman, D. M., Tyson, J. A., Kirkman, D., Dell’Antonio, I., & Bernstein, G. 2000, *Nature*, 405, 143

Zhan, H., & Knox, L. 2004, *ApJ*, 616, L75